

## Aerodynamics of a cylinder in the wake of a V-shaped object

Sangil Kim<sup>1a</sup>, Md. Mahbub Alam<sup>\*2,3</sup> and Mohammad Russel<sup>4b</sup>

<sup>1</sup>Department of Mechanical Engineering, Kangwon National University, 346 Jungang-ro, Samcheok 25913, Republic of Korea

<sup>2</sup>Institute for Turbulence-Noise-Vibration Interaction and Control, Shenzhen Graduate School, Harbin Institute of Technology, Shenzhen 518055, China

<sup>3</sup>Digital Engineering Laboratory of Offshore Equipment, Shenzhen, China

<sup>4</sup>School of Food and Environment, Key laboratory of Industrial Ecology and Environmental Engineering, Ministry of Education, Dalian University of Technology, Panjin 124221, China

(Received March 3, 2016, Revised June 12, 2016, Accepted June 19, 2016)

**Abstract.** The interaction between two different shaped structures is very important to be understood. Fluid-structure interactions and aerodynamics of a circular cylinder in the wake of a V-shaped cylinder are examined experimentally, including forces, shedding frequencies, lock-in process, etc., with the V-shaped cylinder width  $d$  varying from  $d/D = 0.6$  to 2, where  $D$  is the circular cylinder diameter. While the streamwise separation between the circular cylinder and V-shaped cylinder was  $10D$  fixed, the transverse distance  $T$  between them was varied from  $T/D = 0$  to 1.5. While fluid force and shedding frequency of the circular cylinder were measured using a load cell installed in the circular cylinder, measurement of shedding frequency of the V-shaped cylinder was done by a hotwire. The major findings are: (i) a larger  $d$  begets a larger velocity deficit in the wake; (ii) with increase in  $d/D$ , the lock-in between the shedding from the two cylinders is centered at  $d/D = 1.1$ , occurring at  $d/D \approx 0.95$ -1.35 depending on  $T/D$ ; (iii) at a given  $T/D$ , when  $d/D$  is increased, the fluctuating lift grows and reaches a maximum before decaying; the  $d/D$  corresponding to the maximum fluctuating lift is dependent on  $T/D$ , and the relationship between them is linear, expressed as  $d/D = 1.2 + \frac{1}{e}T/D$ ; that is, a larger  $d/D$  corresponds to a greater  $T/D$  for the maximum fluctuating lift.

**Keywords:** cylinder; lock-in; wake; fluctuating lift force

### 1. Introduction

The vortices rotating in opposite directions are generated alternately in two rows due to boundary layer separation from bluff body submerged in a fluid flow. The two rows of vortices are formed in the wake of the body, called Karman vortex streets. In the past, there have been many studies done on Karman Vortex Streets. For example, Griffin and Ramberg (1974) conducted a detailed investigation on the vortex location and circulation, using visualization experiments at

---

\*Corresponding author, Professor, E-mail: [alamm28@yahoo.com](mailto:alamm28@yahoo.com)

<sup>a</sup> Assistant Professor, E-mail: [kimsangil@kangwon.ac.kr](mailto:kimsangil@kangwon.ac.kr)

<sup>b</sup> Assistant Professor, Email: [mrussel@dlut.edu.cn](mailto:mrussel@dlut.edu.cn)

Reynolds numbers  $Re = 144$  and  $190$  for fixed and vibrating cylinders. A structure subjected to a fluid flow may experience vibration due to the Karman vortex shedding from it. On the other hand, the vibration of a structure submerged in the Karman vortex street of another is more complex (Alam and Kim 2009, Kim and Alam 2015). Practical examples in engineering are vibrations of suspension bridges, high-rise buildings, heat-exchanger tubes, risers, etc., due to wind or water flow. The interaction between fluid and structures and its consequence (e.g., vibrations) engender noises, lock-in, resonance, galloping, etc. It is well known that vibration of a structure may result from a lock-in phenomenon where the frequency of vortex shedding from the structure is the same as the natural frequency of the structure. The lock-in phenomenon leads to a resonance, affecting the service life of the structure. An exemplary incident caused by this lock-in phenomenon is the collapse of the Tacoma Bridge in Tacoma in the state of Washington, USA in November 1940. Since then, there have been regularly published studies on vibrating structures subjected to fluid flow.

Dekhordi *et al.* (2011) examined numerically the flow over two identical-diameter tandem cylinders at both laminar and turbulent flow regime. Lam and To (2003) performed an experimental study of two tandem cylinders where the downstream cylinder was flexible, smaller in diameter compared to the upstream cylinder. No violent vibration was observed because the upstream cylinder of being a larger diameter shelters the downstream cylinder. Rahmanian *et al.* (2014) performed a numerical simulation on vortex-induced vibrations of two cylinders that were mechanically coupled, behaving as one combined cylinder. The interaction between the coupled cylinders leads to a very irregular vibration of the bundle both in-line and cross-flow directions. Mahir and Rockwell (1996) studied flow structures around two cylinders vibrated forcibly in-phase and out-of-phase modes. Kim *et al.* (2009a, b) investigated the flow-induced vibration characteristics of two circular cylinders in tandem arrangement and classified the response characteristics of the cylinders into five regimes based on the spacing ratio. Haniu *et al.* (2009) employed forced rotational vibration of a triangular prism to experimentally investigate the transient phenomenon from no-lock-in state to lock-in state. It is of fundamental interest to know the answers to some crucial questions: how does the lock-in of a structure behave when the structure is placed in vortex streets formed by another structure varied in size? How would the street and lock-in influence the fluctuating forces on the structure?

To mitigate the above curiosity, this paper aims to identify the lock-in phenomenon and measure the fluctuating fluid force acting on a circular cylinder placed in the wake of an upstream V-shaped cylinder. In order to change the frequency of vortices in the street, the lateral dimension  $d$  of the V-shaped cylinder was changed systematically from  $d = 0.6D$  to  $2.0D$ , where  $D$  is the circular cylinder diameter. Here we use a V-shaped cylinder as the upstream cylinder so that its width can be changed conveniently. The position of the circular cylinder was varied from the V-shaped cylinder wake centerline ( $T/D = 0$ ) to  $T/D = 1.5$ , where  $T$  is lateral spacing between the circular cylinder center to the V-shaped cylinder wake centerline. While the frequency of vortices generated by the V-shaped cylinder was estimated from a power spectral density function of streamwise velocity obtained using a hotwire, the fluctuating force on the circular cylinder was measured using a sectional load cell.

## 2. Experimental details

The experiments were conducted in a closed-circuit wind tunnel having a test section of 300

mm in width, 1200 mm in height and 2200 mm in length. The free-stream velocity,  $U_0$ , in the tunnel was 10 m/s, giving a Reynolds number ( $Re$ ) of  $3.4 \times 10^4$ , based on  $U_0$  and the circular cylinder diameter  $D$ . Within the test-section, the flow was uniform within  $\pm 2\%$  of the centerline velocity. The longitudinal turbulence intensity, when the tunnel was empty, was less than 0.5% at flow velocity 10 m/s.

Fig. 1 shows the models, experimental arrangement, symbol definitions and the details of the load cell used for fluid force measurement. As seen, the upstream cylinder, V-shaped, was made with two plates, both hinged at the leading edges. Each plate was 50 mm in width and 2 mm in thickness. The circular cylinder placed in the downstream was 50 mm in diameter. Both circular and V-shaped cylinders spanned the horizontal 300 mm dimension of the wind tunnel. The characteristic width of the V-shaped cylinder, defined by  $d$ , is the distance between the two free edges of the plates. Two small rods, each of 10-mm diameter, supported the free edges of the plates, boosting the rigidity of the V-shaped cylinder. Adjustment of the lateral separation between the two rods enables the change in  $d$ . A rectangular coordinate system of  $x$ ,  $y$  and  $z$  corresponding to freestream, cross-stream and spanwise directions, respectively, is adopted with its origin at the intersection of V-shaped cylinder wake centerline and the line connecting centers of the rods.  $z = 0$  corresponds to the midspan of the cylinder.

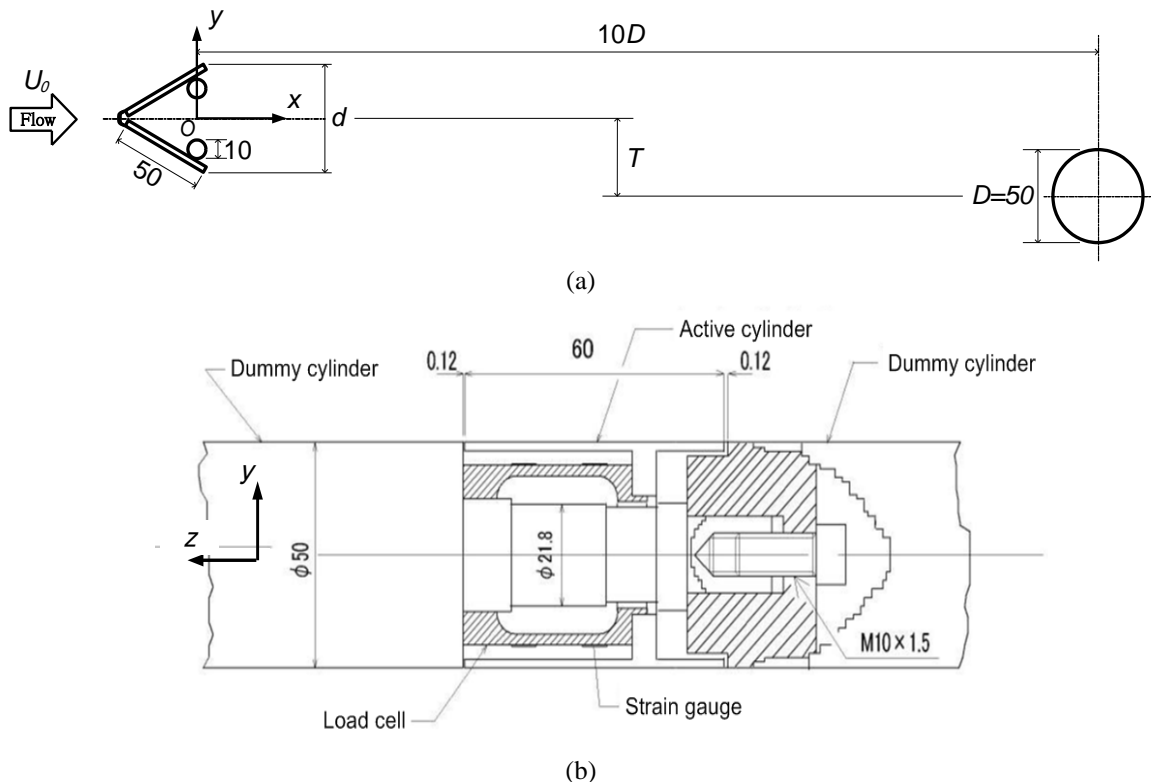


Fig. 1 (a) Models, experimental arrangement and symbol definitions and (b) Details of the load cell installed in the circular cylinder

The circular cylinder was located at  $x = 500$  mm ( $=10D$ ). The lateral spacing between the circular cylinder center and the V-shaped cylinder wake centerline ( $y = 0$ ) is defined by  $T$  (Fig. 1), varied from  $0.0D$  to  $1.5D$ . As the circular cylinder is in the wake of the other, the load cell installed at the midsection of the circular cylinder measured fluctuating forces caused by the convective vortices from the V-shaped cylinder and also by the vortex shedding from the circular cylinder itself. Thus, the power spectrum of fluctuating lift force measured by the load cell can extract vortex shedding frequencies from both V-shaped and circular cylinders. With a change in  $d/D$  from  $0.6$  to  $2.0$  with  $\Delta d/D = 0.1$ , the vortex shedding frequency of the V-shaped cylinder in the absence of the circular cylinder was measured using a hotwire pinpointed at  $(x/D, y/D, z/D) = (10, 1.0, 0)$ . Indeed, the hotwire was traversed from  $y/D = -1.0$  to  $1.8$  (Fig. 2), and the same frequency was detected in the power spectra of the hotwire signals at different  $y/D$ . For two identical-diameter cylinders arranged in tandem, it was found that the shedding frequency of the upstream cylinder is unaffected by the presence of the downstream cylinder when the spacing between the cylinders is larger than  $8D$  (Alam *et al.* 2003, Sumner 2010). So, the presently hotwire-measured frequency of the vortex shedding from the V-shaped cylinder is assumed to be unchanged as the circular cylinder is placed at  $x = 10D$ .

A modal analysis of the fluctuating lift signal is conducted to extract dormant information on lock-in phenomenon and mechanism of maximum lift generation. The fluctuating lift force signal is passed through bandpass filters with pass-band frequencies centered at  $f_1$  and  $f_2$ , where  $f_1$  and  $f_2$  are the shedding frequencies of the upstream and downstream cylinders, respectively. The time-dependent amplitude of the lift is obtained by differentiating the signal; the amplitude corresponds to a slope of zero magnitude. Then the median of the time-dependent amplitude is estimated. When the local amplitude is larger and smaller than the median, the shedding mode is classified as ‘strong’ and ‘weak’, respectively.

### 3. Results and discussion

#### 3.1 The wake of the V-shaped cylinder

Fig. 2 shows the normalized time-mean streamwise velocity  $\bar{u}^*$  ( $=\bar{u}/U_0$ , where  $\bar{u}$  is the time-mean streamwise velocity) in the wake of the V-shaped cylinder at  $x/D = 10$ ,  $y/D = -1.0 \sim 1.8$ , where the width  $d$  of the V-shaped cylinder is changed from  $d/D = 0.6$  to  $2.0$ . Note that the  $\bar{u}^*$  measurements were done in the absence of the circular cylinder, and the  $x/D = 10$  corresponded to the location of the circular cylinder for the two-cylinder measurements. The  $\bar{u}^*$  variation with  $y/D$  for each  $d/D$  is symmetric about  $y/D = 0$ , implying that the wake formed by the V-shaped cylinder is symmetric, as expected. A larger  $d/D$  results in a smaller  $\bar{u}^*$  in the range of  $y/D$  measured, making the wake wider.

#### 3.2 Shedding frequency and fluctuating lift

Fig. 3(a) shows a representative load-cell-measured lift force signal of the circular cylinder for  $d/D = 1.4$  at  $T/D = 0.6$ . The signal consists of two frequencies  $f_1$  and  $f_2$  appearing one after another randomly. For example, a higher frequency  $f_2$  and a lower frequency  $f_1$  prevails in times  $t_1$  and  $t_2$ , respectively (Fig. 3(a)). The power spectrum of the signal, shown in Fig. 3(b), extracts the two

frequencies marked as Strouhal number  $St_1 (= f_1 \cdot D/U_0) = 0.09$  and  $St_2 (= f_2 \cdot D/U_0) = 0.13$ , respectively. It will be confirmed later that  $St_1$  stems from the alternating impingement of convective vortices from the upstream cylinder, and  $St_2$  is the vortex shedding from the downstream cylinder. The values of the two  $St$  are different because the upstream and downstream cylinders are of (i) different characteristic width,  $1.4D$  and  $D$ , respectively, (ii) different local (at the cylinder locations) initial velocities,  $U_0$  and  $0.6U_0$  (Fig. 2), and (iii) different cross-sections, V-shaped and circular.

Fig. 4 displays  $St$  extracted from the lift force signal (circle symbol) and hotwire signal (triangle symbol). Note that the  $St$  measured by the hotwire corresponds to the frequency of vortex shedding from the upstream cylinder, with the hotwire located at  $x/D = 10$ ,  $y/D = 1.0$  in the absence of the downstream cylinder. On the other hand,  $St$  measured by the load cell represents vortex shedding frequencies for both upstream and downstream cylinders. Thus, the two measurements facilitate identifying the phenomenon of lock-in (if any) between the sheddings from the two cylinders. Fluctuating lift coefficient  $C_{L_f}$  of the downstream cylinder might be linked to the upstream cylinder shedding, downstream cylinder shedding, lock-in and  $T/D$ , hence it is superimposed over  $St$  in Fig. 4 as  $C_{L_f}/C_{L_f0}$  ( $\times$  symbol), following the right vertical axis, where  $C_{L_f0}$  is the fluctuating lift in the absence of the upstream cylinder or  $T/D = \infty$ . Interestingly, two Strouhal numbers ( $St_1$  and  $St_2$ ) are generally identified from the load cell measurement: one ( $St_1$ ) equals to that from the hotwire, decreasing with  $d/D$ ; and the other ( $St_2$ ) is much less sensitive to  $d/D$ , nestling in 0.12 - 0.17. The decrease in  $St_1$  is caused by the increase in the bluff width of the upstream cylinder, as a larger  $d$  means a smaller shedding frequency, given the same  $U_0$ .

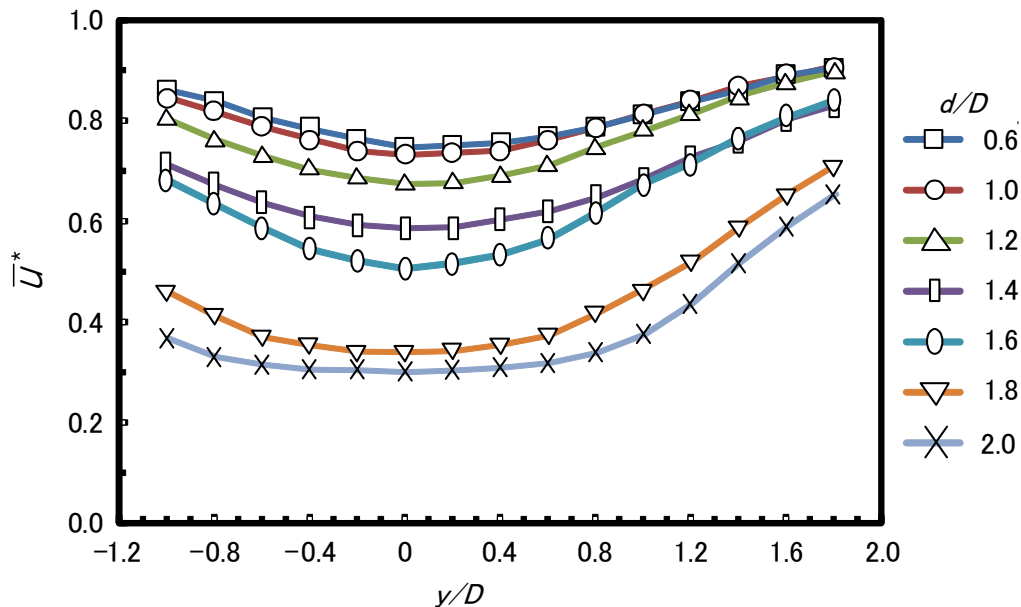


Fig. 2 Normalized streamwise velocity  $\bar{u}^*$  ( $= \bar{u}/U_0$ ) dependence on  $y/D$  and  $d/D$

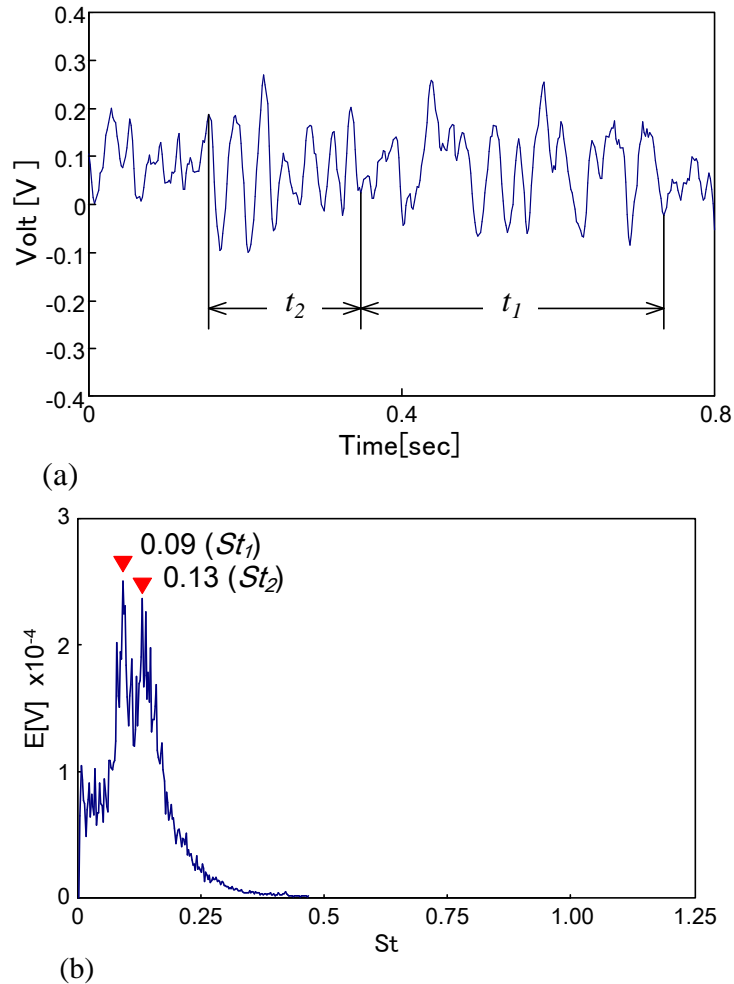


Fig. 3 (a) Time-history of lift force from load-cell, and (b) power spectrum of the lift force signal.  $T/D = 0.6$ ,  $d/D = 1.4$

When  $St_1$  and  $St_2$  are close, a lock-in between the two is observed, with  $St_1$  being modified to  $St_2$ . That is, the downstream cylinder shedding influences the upstream cylinder shedding to be locked-in. The lock-in regime widens up to  $T/D = 0.7$  and then shrinks. Interestingly, the lock-in regime for each  $T/D$  centers at  $d/D = 1.1$ . In other words, the lock-in occurs when the upstream cylinder diameter is 10% bigger than the downstream, i.e., at certain upstream-cylinder wake width or certain lateral width of the two rows of vortices from the upstream cylinder. On the other hand, the downstream cylinder is immersed in the wake of the upstream cylinder; the initial velocity at the downstream cylinder location is much smaller than that at the upstream cylinder. Therefore, a larger  $d$ , compared to  $D$ , is required to make  $St_1$  and  $St_2$  close to each other. Another feature in Fig. 4 is that  $C_{L_f}/C_{L_f0}$  growing with  $d/D$  reaches a maximum value after the lock-in. The  $d/D$  corresponding to the maximum  $C_{L_f}/C_{L_f0}$  is greater for a larger  $T/D$ .

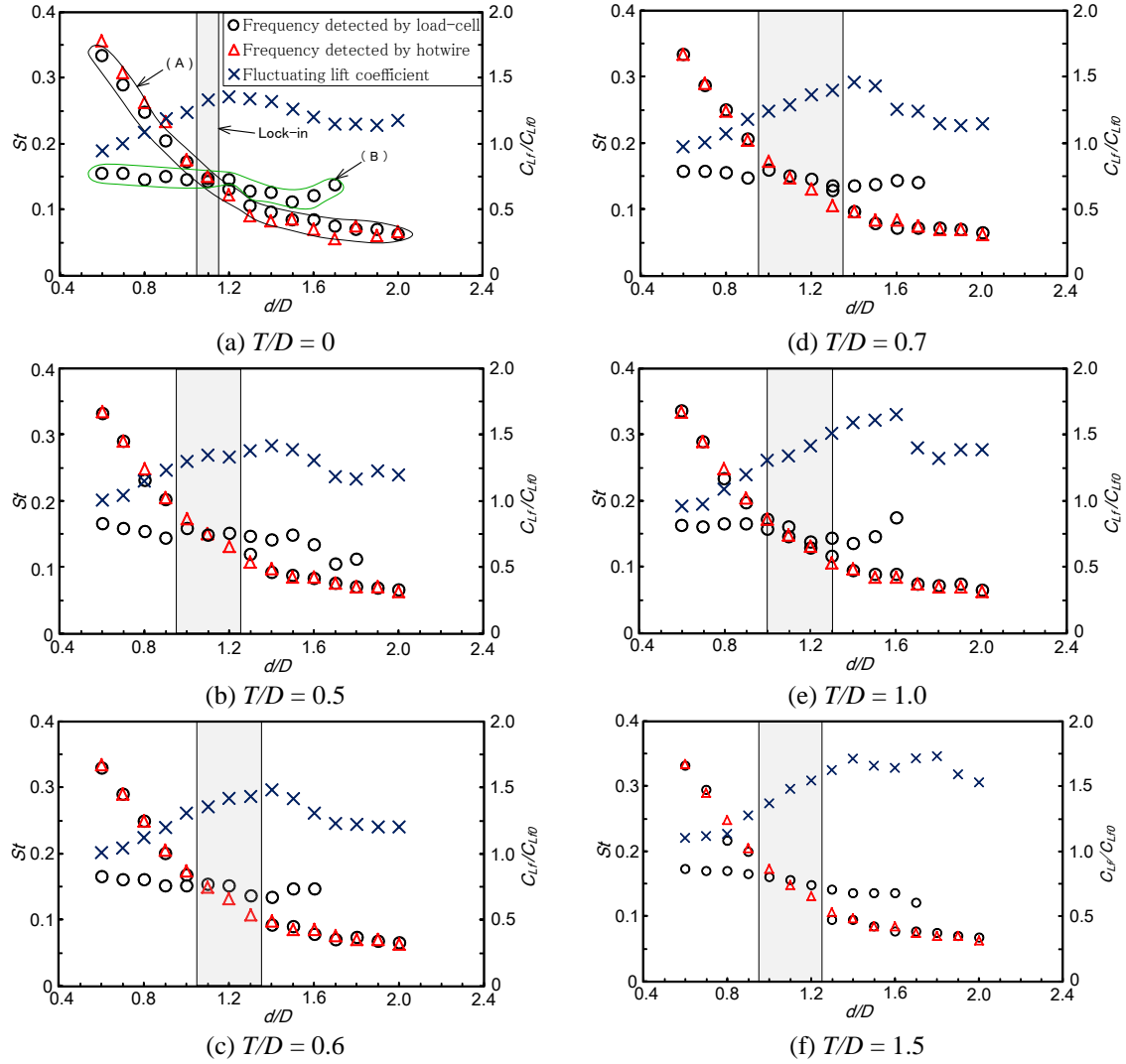


Fig. 4 Strouhal number  $St$  from hotwire (triangle) and load cell (circular symbol) output and fluctuating lift coefficient  $C_{Lf}/C_{Lf0}$ .

In order to explore the global features of  $C_{Lf}/C_{Lf0}$ , a contour plot of  $C_{Lf}/C_{Lf0}$  is rendered as functions of  $T/D$  and  $d/D$  in Fig. 5. The features can be outlined as follows. (1) The thick solid line drawn represents the maximum  $C_{Lf}/C_{Lf0}$  at each  $T/D$ ; hereafter it is dubbed as the critical line. The line suggests that a large  $T/D$  requires a large  $d/D$  corresponding to a maximum  $C_{Lf}/C_{Lf0}$ , with  $d/D$  growing from 1.2 to 1.75 as  $T/D$  extends from 0 to 1.5. The equation of the line can be expressed as,  $d/D = 1.2 + 0.366T/D$ ,  $\Rightarrow d/D = 1.2 + \frac{1}{e}T/D$ . (2) Along the critical line,  $C_{Lf}/C_{Lf0}$  boosts, connected to a stronger interaction between the downstream cylinder and strong vortices from the

upstream cylinder. The boosting  $C_{L_f}/C_{L_f0}$  might be connected to the strength of the upstream-cylinder-generated vortices and interaction mechanisms between the upstream-cylinder-generated vortices and the downstream cylinder (Alam 2014). (3) The lock-in regime, hatched area, appears before the critical line. (4) At  $d/D < 1.0$ ,  $C_{L_f}/C_{L_f0}$  is weakly sensitive to  $T/D$ . So is at  $d/D > 1.5$ ,  $T/D < 0.8$ . The two regimes have different physics. In the former regime, weaker vortices are shed from the upstream, smaller cylinder. The interaction between the upstream-cylinder-generated vortices and the downstream cylinder is thus weak, leading to a very smaller variation with  $T/D$  or  $d/D$ . On the other hand, in the latter regime the upstream cylinder being much larger than the other engenders a larger lateral distance between the two rows of vortices; the downstream cylinder thus lies between the two rows, failing to have a strong interaction with the upstream-cylinder-generated vortices.

### 3.3 Intermittent lock-in between $f_1$ and $f_2$

In order to clarify the influence of intermittent lock-in and non-lock-in, the lift force signal was band passed at 15-20 Hz and 25-30 Hz, corresponding to the upstream and downstream cylinder frequencies ( $f_1$  and  $f_2$ ). Shown in Fig. 6(a, b) at  $T/D = 0.7$ ,  $d/D = 1.4$  are (i) fluctuating lift signal, (ii) time-dependent lift amplitude, (iii) histogram of the lift amplitude, and (iv) timing chart of the presences of strong and weak amplitude corresponding to strong and weak interactions or shedding; here ‘strong’ (set as 1.0) and ‘weak’ (set as -1.0) refer to the cases where the lift amplitude larger and smaller than the median value. Figs. 6(a(iv)) and 6(b(iv)) illustrate that strong and weak modes appear intermittently in the combinations shown in Table 1. The combinations are referred to as modes A, B, C and D. More clearly, mode A means the upstream-cylinder-generated convective vortices approaching the downstream cylinder and the vortices from the downstream cylinder itself both are strong. The former is weaker in mode B, which is considered as the case where the  $f_1$  is absent; that is, the upstream cylinder shedding frequency locks-in to the downstream cylinder. So is the latter in mode C, which is deemed as the lock-in occurring reversely. Both are weak in mode D, weak interactions.

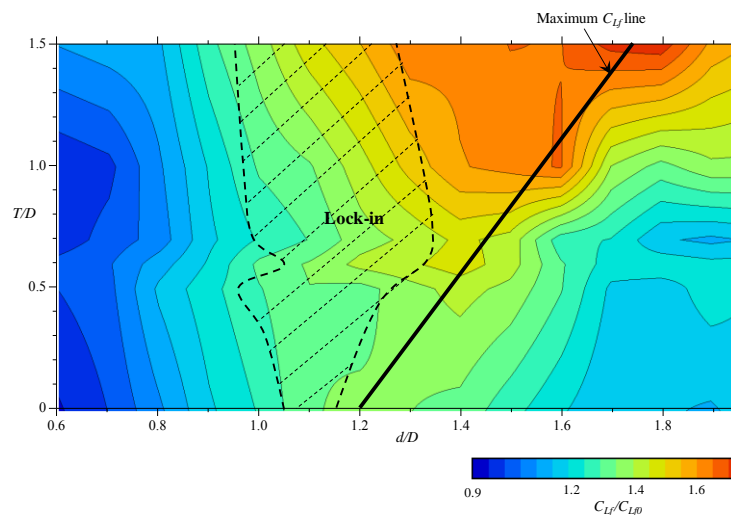
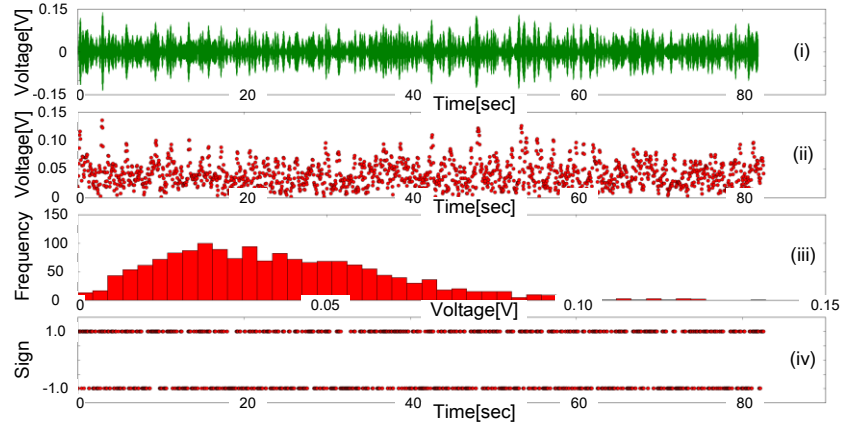
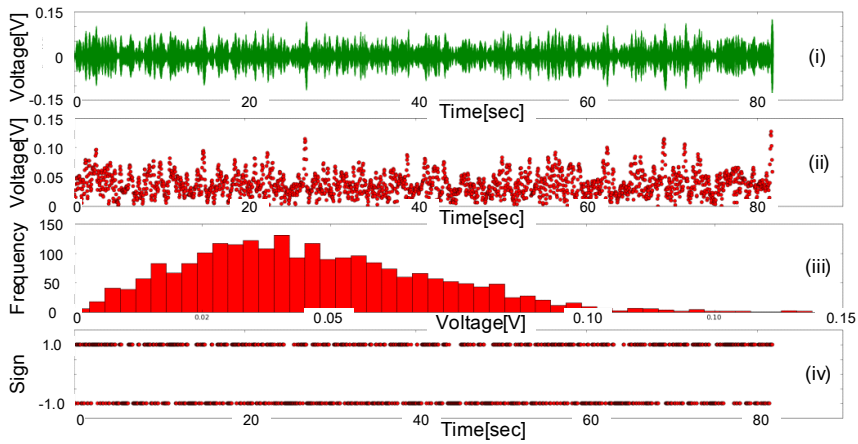


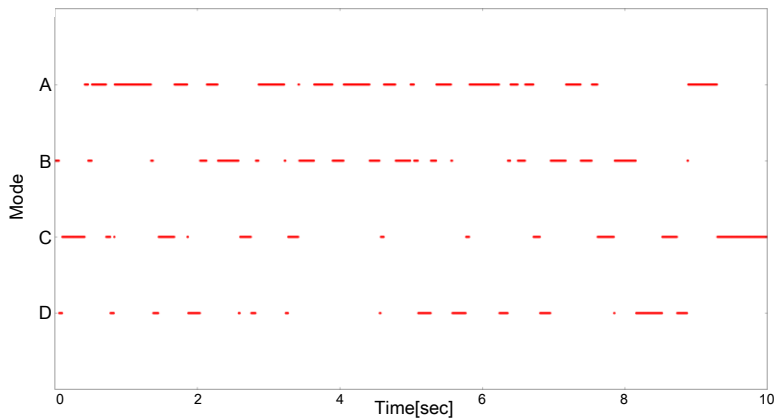
Fig. 5 Contour plot of  $C_{L_f}/C_{L_f0}$  as functions of  $d/D$  and  $T/D$



(a) Frequency  $f_1$  of upstream object



(b) Frequency  $f_2$  of downstream cylinder



(c) Timing chart

Fig. 6 Mode analysis results at  $T/D=0.7$ ,  $d/D=1.4$ . For the definitions of modes A, B, C and D, see Table 1

Table 1 Appearance of modes corresponding to strong and weak in the two frequencies

Frequency $f_1$	Frequency $f_2$	Modes
Strong	Strong	A
Weak	Strong	B
Strong	Weak	C
Weak	Weak	D

Table 2 Appearance of the four Modes at each  $T/D$  ( $d/D=1.4$ )

$T/D$	Mode A [%]	Mode B [%]	Mode C [%]	Mode D [%]
0	29.0	22.1	26.8	22.1
0.5	25.9	23.7	26.6	23.8
0.6	22.0	25.8	26.5	25.7
0.7	38.6	22.6	22.4	16.4
1.0	22.3	21.9	23.5	32.3
1.5	28.9	21.9	22.7	26.5

A timing chart of the four modes following Table 1 and Figs. 6 (a(iv), b(iv)) is presented in Fig. 6(c). Mode A appears more frequently, while mode D appears seldom with an intermediate presence of modes B and C. It can be said that as the interaction for a given  $d/D$  would be contingent on  $T/D$ , the mode analysis is done for  $T/D = 0, 0.5, 0.6, 0.7, 1.0$ , and  $1.5$ , and the results are summarized in Table 2. The prevalence of modes B and C is comparable to each other and about 50% in total. On the contrary, that of modes A and D makes the difference, varying oppositely. At  $d/D = 1.4$ ,  $C_{L_f}/C_{L_f0}$  is found to increase up to  $T/D = 0.6$  (Fig. 5), here the occurrence of mode B is observed to boosts (Table 2) at  $T/D \leq 0.6$ . The observation implies that the longer prevalence of the mode B partially contributes to the increase in  $C_{L_f}/C_{L_f0}$ . Interestingly, at  $T/D = 0.7$  corresponding to the maximum  $C_{L_f}$  for  $d/D = 1.4$  (i.e., the intersection of  $d/D = 1.4$  and the critical line), mode A appears longest (38% of the total time), while mode D appears shortest (16.4%) and modes B and C emerge 22.6% and 22.4%, respectively. That is, the maximum  $C_{L_f}$  is mainly due to mode A.

#### 4. Conclusions

The interaction between a V-shaped upstream cylinder (width  $d$ ) and a circular downstream cylinder (diameter  $D$ ) is examined with measurements of shedding frequency and fluctuating lift force. While  $d$  is varied from  $d/D = 0.6$  to  $2.0$ , the downstream cylinder located at a constant streamwise distance  $x = 10D$  from the upstream cylinder is laterally displaced systematically from  $T/D = 0$  to  $1.5$ . Furthermore, a velocity measurement of the upstream cylinder wake in the absence of the downstream cylinder is done in order to extract the information on how the  $d$  influences the wake. When  $d/D$  is increased, the wake becomes wider, and a larger velocity deficit in the wake of the V-shaped cylinder is observed. The downstream cylinder experiences a lock-in for  $d/D \approx 0.95 - 1.35$  depending on  $T/D$ . The lock-in regime is however centered at  $d/D \approx 1.1$ . For each  $T/D$ , with

an increase in  $d/D$ ,  $C_{L_f}/C_{L_{f0}}$  grows, becomes a maximum at a  $d/D$  beyond the lock-in and then declines. The  $d/D$  corresponding to the maximum  $C_{L_f}/C_{L_{f0}}$  is dependent on  $T/D$ , greater for a larger  $T/D$ , following a critical line  $d/D = 1.2 + \frac{1}{e} T/D$ . Along the critical line,  $C_{L_f}/C_{L_{f0}}$  is enhanced due to a stronger interaction between the downstream cylinder and strong vortices from the upstream cylinder. At  $d/D < 1.0$ ,  $C_{L_f}/C_{L_{f0}}$  is small and weakly sensitive to  $T/D$  because of relatively weaker vortices in the gap between the cylinders. The interaction between the upstream-cylinder-generated vortices and the downstream cylinder is thus weak. At  $d/D > 1.5$ ,  $T/D < 0.8$ , again  $C_{L_f}/C_{L_{f0}}$  is small as the downstream cylinder is submerged in the wake of the upstream larger cylinder, failing to have a strong interaction with the upstream-cylinder-generated vortices. Beyond the lock-in, an intermittent lock-in takes place and contributes to an increase in  $C_{L_f}/C_{L_{f0}}$ .

## Acknowledgments

Kim wishes to acknowledge the support given to him by 2015 Research Grant from Kangwon National University through grants 201510057. Alam wishes to acknowledge supports given to him from the Research Grant Council of Shenzhen Government through grants KQCX2014052114423867 and JCYJ20120613145300404.

## References

- Alam, M.M. (2014), "The aerodynamics of a cylinder submerged in the wake of another", *J. Fluid. Struct.*, **51**, 393-400.
- Alam, M.M. and Kim, S. (2009), "Free vibration of two identical circular cylinders in staggered arrangement", *Fluid Dynam. Research*, **41**(3), 035507.
- Alam, M.M., Moriya, M., Takai, K. and Sakamoto, H. (2003), "Fluctuating fluid forces acting on two circular cylinders in a tandem arrangement at a subcritical Reynolds number", *J. Wind Eng. Ind. Aerod.*, **91**, 139-154.
- Dehkordi, B.G., Moghaddam H.S. and Jafari, H.H. (2011) "Numerical simulation of flow over two circular cylinders in tandem arrangement", *J. Hydrodynamics*, **23**(1), 114-126.
- Griffin, O.M. and Ramberg, S.E. (1974), "The vortex-street wakes of vibrating cylinders", *J. Fluid Mech.*, **66**(3), 553-576.
- Haniu, H., Kim, S., Miyakoshi, K., Takai, K. and Islam, M.R. (2009), "Transitional characteristics of phase shift in lock-in phenomena of an oscillating cylinder", *J. Fluid Sci. Technol.*, **4**(3), 479-489.
- Kim, S., Alam, M.M., Sakamoto, H. and Zhou, Y. (2009a), "Flow-induced vibration of two circular cylinders in tandem arrangement. Part 1: characteristics of vibration", *J. Wind Eng. Ind. Aerod.*, **97**(5-6), 304-311.
- Kim, S., Alam, M.M., Sakamoto, H. and Zhou, Y. (2009b), "Flow-induced vibration of two circular cylinders in tandem arrangement. Part 2: suppression of vibrations", *J. Wind Eng. Ind. Aerod.*, **97**(5-6), 312-319.
- Kim, S. and Alam, M.M. (2015), "Characteristics and suppression of flow-induced vibrations of two side-by-side circular cylinders", *J. Fluid. Struct.*, **54**, 629-642.
- Lam, K.M. and To, A.P. (2003), "Interference effect of an upstream larger cylinder on the lock-in vibration of a flexibly mounted circular cylinder", *J. Fluid. Struct.*, **17**(8), 1059-1078.
- Mahir, N. and Rockwell, D. (1996), "Vortex formation from a forced system of two cylinders. Part I: tandem arrangement", *J. Fluid. Struct.*, **10**(5), 473-489.
- Rahmanian, M., Cheng, L., Zhao, M. and Zhou, T. (2014), "Vortex-induced vibration and vortex shedding

characteristics of two side-by-side circular cylinders of different diameters in close proximity in steady flow”, *J. Fluid. Struct.*, **48**, 260-279.

Sumner, D., Price, S.J. and Paidoussis, M.P. (2000), “Flow-pattern identification for two staggered circular cylinders in cross-flow”, *J. Fluid Mech.*, **411**, 263-303.

**Nomenclature**

$C_{L_f}$	: fluctuating lift coefficient
$C_{L_f0}$	: fluctuating lift coefficient of the circular cylinder in the absence of the upstream object
$d$	: width of the V-shaped cylinder [mm]
$D$	: diameter of circular cylinder [50 mm]
$e$	: natural logarithm [2.71828...]
$E$	: load cell output voltage [V]
$f_1$	: vortex shedding frequency of the V-shaped cylinder [Hz]
$f_2$	: vortex shedding frequency of the circular cylinder [Hz]
$Re$	: Reynolds Number ( $U_0 \cdot D / \nu$ )
$St$	: Strouhal number
$T$	: lateral distance between the two cylinders [mm]
$U_0$	: freestream flow velocity [m/s]
$u$	: streamwise velocity [m/s]
$\bar{u}^*$	: normalized time-mean streamwise velocity
$\bar{u}$	: time-mean streamwise velocity
$\nu$	: kinematic viscosity of air
$(x, y)$	: Cartesian coordinate system [mm]